Synthesis and Characterization of Poly(ε-caprolactone-*b*-4-vinylpyridine): Initiation, Polymerization, Solution Morphology, and Gold Metalation

Chu-Hua Lu,[†] **Chih-Feng Huang,**[†] **Shiao-Wei Kuo,**[‡] **and Feng-Chih Chang*,**[†]

Institute of Applied Chemistry, National Chiao Tung University, 30010 Hsinchu, Taiwan, and Department of Materials and Optoelectronic Science, Center for Nanoscience and Nanotechnology, National Sun Yat-Sen University, 804 Kaohsiung, Taiwan

ABSTRACT: We have synthesized a difunctional initiator—the hydroxyl-4-oxo-*N*-alkoxyamine (**HOA**)—by first mixing benzoyl peroxide (BPO) and 4-hydroxyl-2,2,6,6-tetramethylpiperdinooxy (4-OH-TEMPO) in styrene at temperatures below 25 °C to give the 4-oxo-*N*-alkoxyamine (**OA**) and then hydrolyzing the benzoate ester on **OA** with NaOH. This low-temperature preparation of **OA** reveals that benzyloxyl radicals can be generated from the BPO through redox reaction with 4-OH-TEMPO as well as through thermal decomposition. The *N*-oxoammonium cation (i.e., the oxidative state of 4-OH-TEMPO), which formed as a side product, mediated the alcohol oxidation to give **OA**. We prepared three PCL-*b*-P4VP diblock copolymers (**BC1−3**) from **HOA** through two-step polymerizations: (i) diethylaluminum alkoxide-induced ring-opening polymerization of ε-caprolactone at 25 °C followed by (ii) nitroxide-mediated radical polymerization of 4-vinylpyridine at 125 °C. With the combination of biodegradable hydrophobic PCL blocks and polymeric blocks of P4VP ligands, we used the immiscible PCL-*b*-P4VP copolymers to transport $AuCl_4^-$ anions from aqueous phases to organic phases and to stabilize Au nanoparticles in the PCL-*b*-P4VP micelles **Au-BC1−3** after reduction with $NaBH_4$.

Introduction

Diblock copolymers comprising two dissimilar blocks can form two separate and thermodynamically stable microstructures in the bulk state. The hydrophilic side groups of amphiphilic diblock copolymers are highly permeable to water[1–6] or can be selectively removed to create nanopores for water passage.[7,8] When placed in a solvent that solvates only one of the components well, diblock copolymers self-assemble into core/shell micellar microstructures in which the insoluble block comprises the core, thereby avoiding contact with the solvent.[9] In their pioneering research, Eisenberg and co-workers observed that micelles formed from linear diblock copolymers in several morphologies, including spheres, rods, vesicles, and large compound micelles.[10–12] Depending on the molecular masses of the two blocks, the sizes of micelles can range from 10 to 1000 nm, providing a large contact area for two-phase extraction of metal ions: one block to capture metal ions from water in the insoluble cores and the other to stabilize the micelles in organic solvent. Metal-binding polymers are usually amphiphilic because of the need for highly polar interactions (e.g., ionic bonds) between the metal ions and the polymer. Therefore, hydrophobic nonmetallic PCL block is necessary to form the shells of diblock copolymer micelles in organic solvent while P4VP block captured metal ions from aqueous phase or protecting metal nanoparticles after reduction for two-phase extraction of metal ions. Biodegradable and biocompatible polymers are better choices for use as shell components, i.e., to minimize the use of chemicals and the impact on the environment.[1] For example, poly(ε-caprolactone-*block*-4-vinylpyridine) (PCL-*b*-P4VP) is such a diblock copolymer that forms core/shell micelle structures in toluene.[13]

Gold nanoparticles (Au NPs)[14] have recently found many applications in industrial chemistry, such as in low-temperature CO oxidation,[15,16] hydrocarbon hydrogenation,[17–19] low-temperature hydrocarbon oxidation,[20,21] and NO reduction.[22] Most Au NPs are prepared through the chemical reduction of tetrachloroaurate ($AuCl_4^-$) using reducing agents such as sodium borohydride,[23] hydrazine,[24] or lithium borohydride.[25] The protonated pyridyl nitrogen atoms of P4VP blocks form ionic bonds with $AuCl_4^-$ ions, and they also coordinate to the Au NPs formed after reduction of these ions.[24–27] Thus, PCL-*b*-P4VP copolymer micelles can be prepared to capture $AuCl_4^-$ ions from water and to recycle Au NPs into organic solvents.

PCL-*b*-P4VP copolymers can be synthesized through ring-opening polymerization (ROP) of ε-caprolactone (ε-CL) followed by free radical polymerization (FRP) of 4-vinylpyridine (4-VP). After ligand exchange of the hydroxyl groups with either stannous(II) octoate [Sn(Oct)₂] or aluminum tris(isopropoxide) [Al(iOPr)₃], the stannous alkoxide group (SnOR) can catalyze the bulk ROP of ε-CL at 110 °C or the aluminum alkoxide group (Al-OR) can initiate ROP of ε-CL at 25 °C in toluene or tetrahydrofuran.[28,29] Living free radical polymerizations (LFRPs) exhibiting low degrees of radical termination are necessary for polymerization of the second P4VP block from the PCL macroinitiator.[30] In such LFRPs as atom transfer radical polymerization (ATRP), nitroxide-mediated radical polymerization (NMRP), and reversible addition−fragmentation (RAFT), the propagating radicals P• react reversibly with inert persistent species T [e.g., a Cu(I) complex for ATRP, a stable nitroxide free radical (e.g., TEMPO or 4-OH-TEMPO in this study) for NMRP, or a dithioate for RAFT] to form reversible dormant products (P-T), significantly increasing the selectivity ($r_p/r_t =$ ca. 1/[P•]) of propagation ($r_p =$ ca. [P•]) to termination ($r_t =$ ca. [P•]²), where r_p, r_t, and [P•] are the rates of propagation and termination and the concentration of the propagation radical, respectively.[31–33] Because the strong metal ligands of the P4VP block react with copper cations to form metal complexes during ATRP, purification of the resulting polymers can be very time-consuming and repetitious. Using the RAFT technique, the dithioate reagents can bond with the metal ions. Thus, it is not easy to incorporate dithioate groups onto the chain end of PCL

* To whom corresponding should be addressed: e-mail changfc@mail.nctu.edu.tw; Tel 886-3-5131512; Fax 886-3-5131512.
† National Chiao Tung University.
‡ National Sun Yat-Sen University.

Scheme 1. Synthetic Route toward NMRP through BPO−TEMPO Bimolecular Initiation: (a) *N*-Alkoxyamine Initiator Formation; (b) Styrene Monomer Insertion
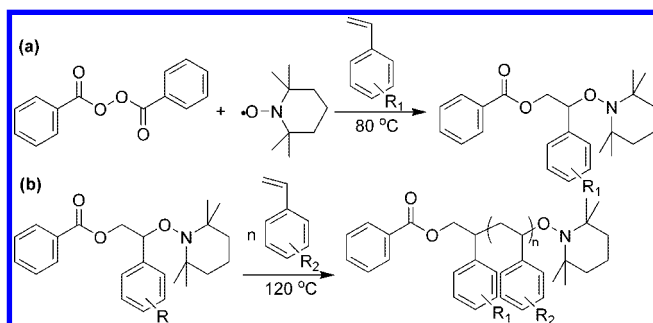
for preparation of PCL-*b*-P4VP block copolymers. The use of styrenic monomers, a unimolecular initiator, and bulk polymerization are the three major limitations of the TEMPO-mediated NMRP because of the high dissociation energy of the C−O bonds on the *N*-alkoxyamine groups, the high reactivity of TEMPO, and the ready transfer of the free radicals to the solvent. In the absence of a metal catalyst, NMRP remains the preferable route toward PCL-*b*-P4VP copolymers.[34] Moreover, Hawker et al. succeeded in the preparation of poly(ε-caprolactone-*block*-styrene) through the ROP of ε-CL and the NMRP of styrene when using hydroxyl-functionalized *N*-alkoxyamines (the same structure as **HA** in this study) as difunctional initiators.[35]

During the propagation step of TEMPO-mediated NMRPs using a starting material of benzoyl peroxides (BPOs) at 120 °C, a vinyl monomer is inserted into the C−O bond of the *N*-alkoxyamine end group (Scheme 1b), which arises as the product of the radical addition between a carbon-centered radical and TEMPO (Scheme 1a). Such *N*-alkoxyamine products are stable at temperatures below 50 °C, and thus, they can be isolated for use as unimolecular initiators for one-step polymerizations at 120 °C.[36] In contrast, the in-situ preparation of *N*-alkoxyamine intermediates—by mixing a radical source (e.g., BPO or AIBN) and a stable nitroxide free radical (e.g., TEMPO or 4-OH TEMPO)—allows them to be used as bimolecular initiators for two-step polymerizations (e.g., one performed at 80 °C for 2 h and the other at 120 °C for 24 h; Scheme 1). In 1993, it was determined that the optimal TEMPO addition for living polystyrene polymerization was 1.3 equiv relative to BPO (rather than the 2-fold ratio expected theoretically), implying that side reactions occurred for the bimolecular initiator.[37,38] The decomposition temperature (T_d, i.e., the temperature at which half of the concentration is consumed within 1 h) of the BPO is 92 °C in toluene. Thus, the reaction temperature for the preparation of *N*-alkoxyamines using BPO and TEMPO in styrene has been established to be 80 °C. A 42% yield of *N*-alkoxyamine products was obtained after column chromatographic purification at this reaction temperature.[36] Gravert and Janda found, however, that this product was formed in 34% yield at 50 °C.[39] Moad et al.[40,41] and Veregin et al.[42] studied the mechanism of the reaction between BPO and TEMPO in styrene at 60 °C. In addition to the thermolysis of BPO, they found that TEMPO can react with BPO to give the benzoxyloxyl radical, benzoate anion, and *N*-oxoammonium cation through one-electron transfer. Unfortunately, this redox reaction has been studied only rarely, even though NMRP has been applied widely to polymer synthesis since 1993.[37] Many reports mention that high-temperature decomposition of BPO results in radical-induced side reactions and, thus, low yields (<50%) of *N*-alkoxyamine products. We suspected that TEMPO-induced BPO decomposition could be a major reason for this behavior because an equimolar amount of TEMPO is required to prepare the

benzoyoxyl radicals in this reaction pathway. For this purpose, it was necessary to clarify the mechanism of the reaction occurring between BPO and TEMPO in the styrene medium prior to NMRP. Braslau et al. demonstrated many alternative methods for generating carbon-centered radicals at temperatures below 50 °C for preparing high-yield *N*-alkoxyamine products as unimolecular initiators for NMRP; these methods included PbO$_2$-mediated oxidation of benzylhydrazine, Cu^{II}-mediated oxidation of lithium enolates, and hydrogen or halide abstraction with non-carbon-centered radicals formed through photolysis or low-temperature thermolysis.[43] Nevertheless, most polymer chemists still select the BPO−TEMPO initiation system to prepare *N*-alkoxyamine unimolecular initiators because of its low-cost raw materials and simplicity. In addition, the benzoic ester products of *N*-alkoxyamines can be used in many wide-ranging applications after alkaline hydrolysis. Use of the commercially available 4-hydroxyl-TEMPO is another option because the additional hydroxyl unit on the nitroxyl moiety is another group that can be converted into a variety of functionalities through chemical modification. Yin et al. attempted to prepare 4-OH-TEMPO-based *N*-alkoxyamines but found that major products of the 4-hydroxyl-*N*-alkoxyamines were oxidized to 4-oxo-*N*-alkoxyamines, resulting in 8.6% and 18.5% yields for the 4-hydroxyl- and 4-oxo-*N*-alkoxyamines, respectively.[44] Thus, Hawker et al. protected the hydroxyl unit of 4-hydroxyl-TEMPO in the form of its benzoate ester to prepare diol *N*-alkoxyamines for the radical crossover study.[45] Taken together, all of these reports suggest that the reaction mechanism between BPO and TEMPO is worth studying, especially for living free radical polymerizations.

In this study, we synthesized the hydroxyl-functionalized *N*-alkoxyamine **HOA** for use in PCL-*b*-P4VP diblock copolymerizations employing sequential ROP and NMRP procedures in one batch. When preparing the *N*-alkoxyamines **A** and **OA**, heating was unnecessary, but the reaction rates were suppressed upon immersing the flask in an ice bath. The color of the solution changed from reddish brown to pale green initially for the reactions proceeding at temperatures below 25 °C. The comprehensive reaction mechanism was deduced after structural identification of the *N*-alkoxyamine products and their side products. With the stable nitroxide free radical of 4-OH-TEMPO, the product of **HOA** was used to initiate the ROP of ε-CL in toluene at 25 °C after the reaction with triethylaluminum (AlEt$_3$). The PCL-*b*-P4VP copolymers were obtained through bulk NMRP of 4-VP from PCL macroinitiators at 125 °C. Using ^{1}H NMR spectroscopic and GPC analyses, the living behavior of the ROP was confirmed by the linear relationship between the monomer conversion and the polymer molecular mass because all of the monomers were inserted from the aluminum alkoxide (Al−OR) bonds. Two HOA-to-AlEt$_3$ molar ratios (r = 1:1.2 or 1:0.6) were investigated for a kinetic study for the ROP of ε-CL in toluene (v = 30 or 60 mL). When r and v were 1.5 and 30 mL, respectively, the 99.5% conversion of the ε-CL monomers was achieved, and then the solution batch was allowed to proceed via the NMRP of 4-VP at 125 °C after vacuum distillation of toluene. The similar trends in the GPC traces obtained using RI and UV dual detectors provided evidence for the NMRP of 4VP from the PCL macroinitiator, i.e., because only the P4VP blocks absorb UV light. DSC thermograms revealed two glass transition temperatures—i.e., distinct thermal chain motions in the separation microdomains of the PCL and P4VP blocks—confirming that immiscible PCL-*b*-P4VP diblock copolymers had formed. After staining the P4VP cores with RuO$_4$ vapor, TEM images revealed micellar structures for the PCL-*b*-P4VP copolymers in a selective solvent for the PCL block [90% toluene/10% dichloromethane (DCM), v/v]. Although the two blocks of the PCL-*b*-P4VP copolymers
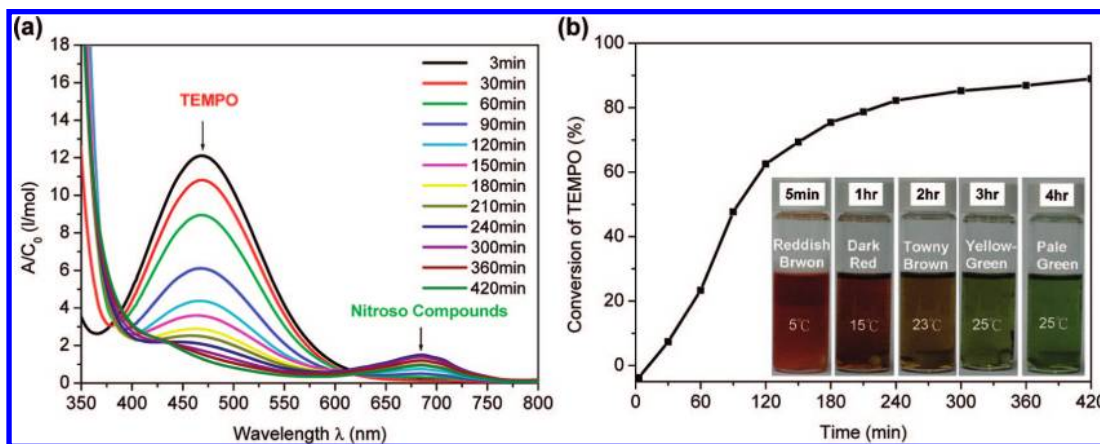
Figure 1. (a) UV−vis spectra and (b) TEMPO conversion of the reaction mixture containing BPO, TEMPO, and styrene at various time intervals during ambient warming from 0 to 25 °C (*A*: UV−vis absorbance; C_0: initial concentration of TEMPO in solution; UV−vis quantification at 469.5 nm).
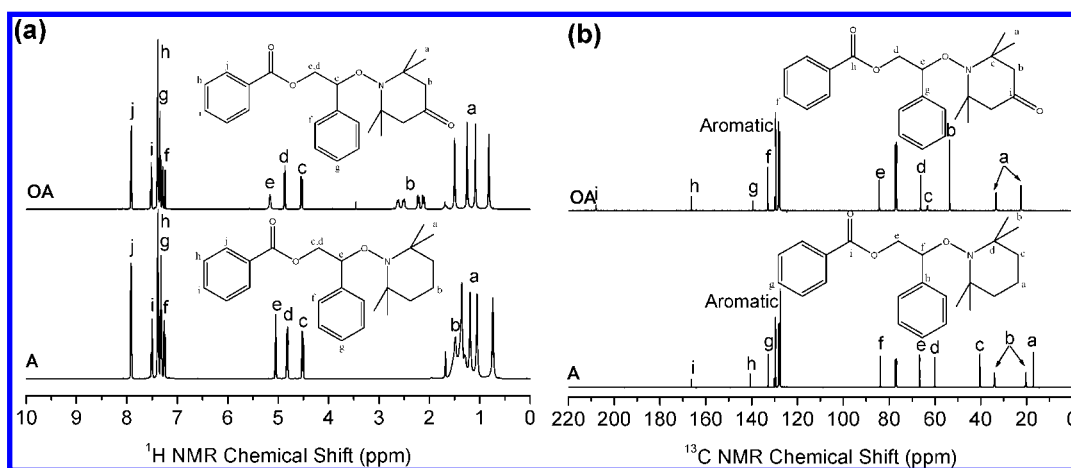

Figure 2. (a) ^{1}H and (b) ^{13}C NMR spectra of the *N*-alkoxyamine **A** and the 4-oxo-*N*-alkoxyamine **OA** formed from the reaction between BPO and TEMPO or 4-OH-TEMPO in styrene at temperatures below 25 °C.

are intrinsically insoluble in water, the P4VP block can capture $AuCl_4^-$ from the water−DCM interface in the form of an ionic pair ($NH^+ \cdots AuCl_4^-$). Upon reduction with aqueous $NaBH_4$ solution, Au NPs were formed in the P4VP block core. As a result, the organic phase became yellow after two-phase extraction but turned red after reduction. After the addition of excess toluene, we used UV−vis spectroscopy, DLS, and TEM to analyze the Au NPs formed through PCL-*b*-P4VP copolymer-mediated reduction in the solvent selective for the PCL block.

Experimental Section

Materials. ε-Caprolactone (ε-CL, 99.5%, ACROS), 4-vinylpyridine (4-VP, 99.5%, ACROS), and toluene (HPLC grade, TEDIA) were dried over calcium hydride (CaH_2, 95%, ACROS) for 24 h and then distilled under reduced pressure. The following chemicals and solvents were used as received: benzoyl peroxide (BPO, >97%, Fluka), styrene (St, 99%, ACROS), 2,2,6,6-tetramethylpiperidinooxy (TEMPO, 98%, ACROS), 4-hydroxy-2,2,6,6-tetramethylpiperidinooxy (4-OH-TEMPO, 98%, ACROS), triethylaluminum ($AlEt_3$, 0.9 M in hexane, Fluka), glacial acetic acid (HPLC grade, TEDIA), cyclopentanol (**1**, 99%, Alfa Aesar), hydrogen tetrachloroaurate(III) trihydrate ($HAuCl_4 \cdot 3H_2O$, 99.9%, ACROS), sodium borohydride ($NaBH_4$, 99.5%, ACROS), cyclohexanol (**2**, 99%, Alfa Aesar), cycloheptanol (**3**, 95%, Alfa Aesar), 1-pentanol (**4**, 98%, ACROS), 2-octanol (**5**, 97%, ACROS), tetrahydrofuran (THF, HPLC grade, TEDIA), methanol (MeOH, HPLC grade, TEDIA), and diethyl ether (Et_2O, HPLC grade, TEDIA). Reactions were performed in glassware under a static atmosphere of argon.

Measurements. ^{1}H and ^{13}C NMR spectra were recorded using a Varian Unityinova 500 NMR spectrometer. Elemental analyses were performed using a Heraeus CHN-O Rapid apparatus (Heraeus VarioEL). MS/MS measurements were performed using an ESI quadrupole time-of-flight instrument (Q-TOF; Micromass) operated in positive ion mode. GC-MS analyses were performed using a Trio 2000 quadrupole mass spectrometer (Micromass, Manchester, UK) equipped with a Fisons Instruments 8060 gas chromatograph and a fused silica capillary column (length: 30 m; inner diameter: 0.5 mm; film thickness: 0.25 μm) from Supelco. EI-MS analyses were performed through continuous quadrupole scanning at an ionization energy of 70 eV. UV−vis spectra were measured using a UV-1601 spectrophotometer (Shimadzu, Japan). Melting points were measured on a Fargo MP-2D apparatus. The weight-average (M_w), number-average (M_n), and maximum (M_v) molecular weights and the polydispersity index (M_w/M_n) were determined through gel permeation chromatography (GPC) using a Waters 510 HPLC, equipped with a 410 differential refractometer, a refractive index (RI) detector, and three Ultrastyragel columns (100, 500, and 103) connected in series in order of increasing pore size, with DMF as eluent at a flow rate of 0.6 mL/min. DLS measurements were performed on a Brookhaven photon correlation spectrometer with BI9000 AT digital correlation. The instrument was equipped with a compass 315M-150 laser (Coherent Technologies), which was operated at a wavelength of 532 nm. Dust-free vials were used for sample preparation at a concentration of 1 mg/mL in a mixture of 10% DCM/90% toluene (v/v); measurements were made at 25 °C at an angle of 90°. The CONTIN algorithm was used to analyze the data. A DuPont DSC-9000 calorimeter, operated at a scan rate
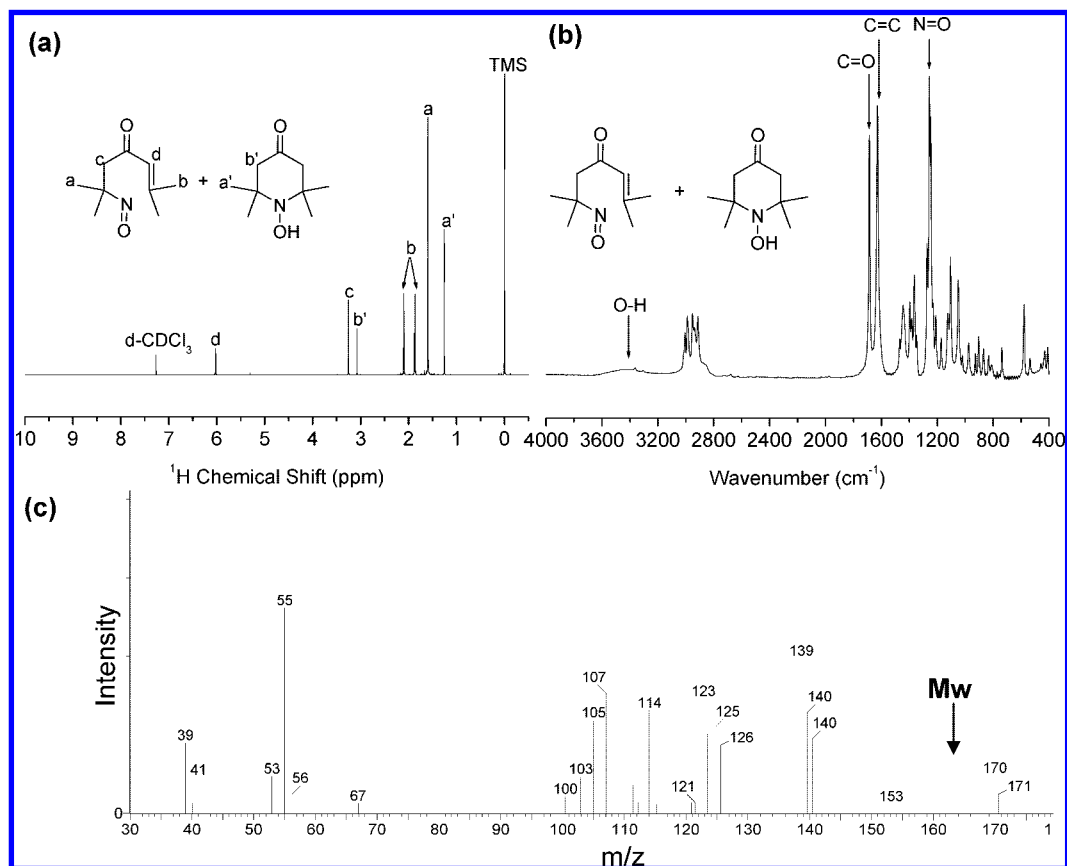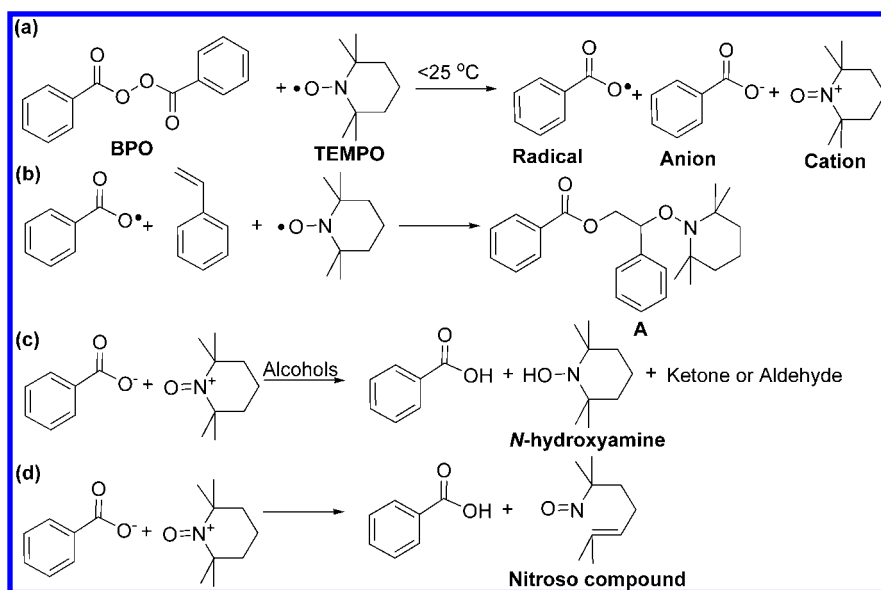
Figure 3. Structural identification of a mixture of *N*-hydroxy-4-oxo-2,2,6,6-tetramethylpiperidine and 2,6-dimethyl-6-nitrosohept-2-en-4-one using (a) ^{1}H NMR and (b) FTIR spectroscopy and (c) mass spectrometry.

Scheme 2. Low-Temperature Reaction Mechanism: (a) Redox-Induced Decomposition of BPO; (b) Radical Addition; (c) Alcohol Oxidation; (d) Ring-Opening Rearrangement

of 20 °C/min over the range from −100 to +180 °C, was used to record the DSC thermograms of samples (ca. 5−10 mg) sealed in aluminum pans. The temperature and energy were calibrated with indium. The glass transition temperature was obtained as the midpoint of the specific heat increment. A TA Instruments thermogravimetric analyzer, operated at a scan rate of 20 °C over temperatures ranging from 30 to 800 °C under a nitrogen purge of 40 mL/min, was used to record TGA thermograms of samples on a platinum holder. A Hitachi H-7500 transmission electron microscope (100 kV) was used to record TEM images of the diblock

copolymer micelles after staining with RuO$_4$ vapor. A drop of dilute solution (1 mg/mL) was placed onto a carbon-coated copper grid. After 3 min, the excess solution was blotted away using a strip of filter paper. The samples were air-dried at room temperature and then stained with RuO$_4$ vapor.

UV−vis Calibration of TEMPO Concentration. The concentration of TEMPO in a reaction mixture can be determined using the Beer−Lambert law ($A = \varepsilon b c$) by monitoring the characteristic UV−vis signal of TEMPO at 469.5 nm. In this equation, A is the absorbance at 469.5 nm in the UV−vis spectrum, ε (L/(mol cm))
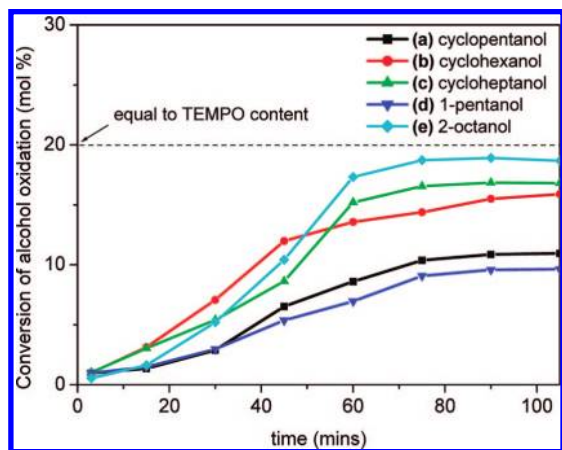
Figure 4. ^{1}H NMR monitoring the alcohol conversion in the reaction mixture: (a) cyclopentanol, (b) cyclohexanol, (c) cycloheptanol, (d) 1-pentanol, and (e) 2-octanol.

is the molar absorptivity of TEMPO in THF, c (mol/L) is the concentration of TEMPO, and b (cm) is the path length of the sample holder. The constant εb was calculated to be 10.59 L/mol from the slope of the linear curve fitting the absorbance to the concentration (Supporting Information, Figure S2). Therefore, the concentration of TEMPO at a given time interval can be deduced from the expression $A/(\varepsilon b)$. To ensure that all data were located on the calibration curve, the reaction mixtures were diluted with THF prior to analysis.

Syntheses of *N*-Alkoxyamines. A solution of BPO (15.0 g, 61.9 mmol) and TEMPO (5.0 g, 32 mmol) or 4-hydroxy-TEMPO (5.5 g, 32 mmol) in styrene (50 mL) was cooled to 5 °C in an ice bath and then naturally warmed to room temperature after a removal of the bath. The reddish-brown solution gradually faded, turning into a pale green solution over several hours. The excess styrene was removed through vacuum distillation, and the residual solid was partitioned between diethyl ether and 1 N aqueous NaOH. The product in the organic phase was dried (anhydrous MgSO$_4$), and the solvent was evaporated to give a light-yellow powder. White crystals of *N*-alkoxyamine products—the *N*-alkoxyamine **A** (5.2 g, 43%) and 4-oxo-*N*-alkoxyamine **OA** (4.3 g, 37%)—were obtained after recrystallization from MeOH. Melting points: **A**, 74.5 °C; **OA**, 111.0 °C. Mass spectra (ESI, *m/z*): **A**, 382.1 [MH$^+$]; **OA**, 396.2 [MH$^+$]. Elem. Anal. for **A** (C$_{24}$H$_{31}$NO$_3$): Calcd: C, 75.56; H, 8.19; N, 3.67; Found: C, 75.66; H, 8.23; N, 3.46; for **OA** (C$_{24}$H$_{29}$NO$_4$): Calcd: C, 72.89; H, 7.39; N, 3.54; Found: C, 72.84; H, 7.45; N, 3.31. ^{1}H and ^{13}C NMR spectra of **A** and **OA** are presented in Figure 2. FTIR spectra of **A** and **OA** are presented in Figures S5 and S6 of the Supporting Information, respectively.

Synthesis of Hydroxyl-*N*-alkoxyamines. 10 N aqueous NaOH (10 mL) was added dropwise to a solution of the *N*-alkoxyamine adduct **A** (5.0 g, 13.1 mmol) or **OA** (5.0 g, 12.6 mmol) in a mixture of THF (10 mL) and MeOH (30 mL). After several hours, the solvent was removed through rotary evaporation, and the product was washed with excess diethyl ether. After rotary evaporation, **HA** (3.3 g, 90%) was obtained as a light-yellow liquid or **HOA** (3.2 g, 87%) was obtained as a white solid (mp 69.2 °C). Mass spectra (ESI, *m/z*): **HA**, 278 [MH$^+$]; **HOA**, 292 [MH$^+$]; Elem. Anal. for **HA** (C$_{17}$H$_{27}$NO$_2$): Calcd: C, 73.61; H, 9.81; N, 5.05; Found: C, 73.79; H, 9.57; N, 4.95; for **HOA** (C$_{17}$H$_{25}$NO$_3$): Calcd: C, 70.07; H, 8.65; N, 4.81, Found: C, 69.96; H, 8.76; N, 5.43. The ^{1}H and ^{13}C NMR spectra of **HA** and **HOA** are presented in Figures S3 and S4, respectively; their FTIR spectra appear in Figures S7 and S8, respectively.

Synthesis of *N*-Alkoxyamine-Functionalized Poly(ε-caprolactone). A solution of AlEt$_3$ (ca. 0.9 mol/L in hexane, 0.42 mL) was added to a solution of hydroxyl-4-oxo-*N*-alkoxyamines (**HOA**, 27.8 mg, 0.25 mmol) in dry toluene (5 mL) under an argon atmosphere. The mixture was stirred at room temperature for 30 min, and then the resultant ethane was removed under reduced pressure. After

adding dry toluene (25 mL), the flask was cooled in an ice bath and then ε-CL (5 mL) was quickly injected into the reaction mixture. The polymerization was performed at 25 °C for a given time and then stopped through the addition of glacial acetic acid (0.2 mL). After evaporation of the toluene through vacuum distillation, the PCL macroinitiator was used directly for the polymerization of 4-VP.

Synthesis of Poly(ε-caprolactone)-*block*-poly(4-vinylpyridine) Copolymers. The dried PCL macroinitiator was charged with 1, 2, or 4 equiv of the 4-VP monomer, based on the content of ε-CL. The vessel was immersed in an oil bath maintained at a temperature of 125 °C. When the stirrer bar stopped stirring in the highly viscous solution, the polymerization was quenched through immersion of the flask in an ice bath. The resultant diblock copolymers **BC1-3** were purified twice through dissolution in chloroform and precipitation from hexane.

Preparation of Micelle Solutions. The diblock copolymer was dissolved DCM, a good solvent for both blocks, at a concentration of 10 mg/mL. Next, a poor solvent for one of the blocks was added to the polymer solution very slowly (up to 90%, v/v) to obtain a desired concentration of 1 mg/mL. Stirring of the solution was continued for 1 h (Figure 7 and Figure 9a) and 24 h (Figure 9b) prior to characterization.

Synthesis of PCL-*b*-P4VP Copolymer-Mediated Au NPs. Equimolar amounts of the pyridine units of the PCL-*b*-P4VP copolymers **BC1-3** in DCM (10 mL) were added to an AuCl$_4^-$ solution (30 mM, 10 mL) under stirring with a magnetic bar stirring. After 1 h, aqueous NaBH$_4$ solution (300 mM, 10 mL) was added, and then the mixture was stirred for another 1 h. The PCL-*b*-P4VP copolymer-protected Au NPs **Au-BC1−3** were stabilized after adding toluene and separating the organic phase.

Results and Discussion

***N*-Alkoxyamines.** In comparison with bimolecular initiation, unimolecular initiation of NMRP provides improved control over the molecular mass distribution with narrow polydispersity ($M_w/M_n < 1.5$). Therefore, we prepared *N*-alkoxyamine unimolecular initiators for the synthesis of PCL-*b*-P4VP diblock copolymers using benzoyl peroxide (BPO) and 2,2,6,6-tetramethylpiperdinooxy (TEMPO) in the styrene medium. We observed, however, abnormal release of heat, resulting in the temperature increasing up to 50 °C, after mixing BPO with TEMPO in the styrene medium at 25 °C. Thus, this exothermic reaction should be suppressed by cooling rather than heating. Because of the low solubility of BPO in styrene at temperatures below 20 °C, we controlled this reaction by dissolving BPO slowly during natural warming at temperatures between 5 and 25 °C. Remarkably, the color of the solution turned from reddish brown to pale green (Figure 1b), indicating consumption of TEMPO (note that reddish brown is the intrinsic color of stable nitroxide free radicals). Monitoring of TEMPO content at regular intervals using UV−vis spectroscopy (Figure 1a), we observed that the nitroxide absorbance at 469.5 nm decreased as the solution's color faded. We determined the conversion of TEMPO quantitatively through calibration with the UV−vis spectra of pure TEMPO in THF; we found that the conversion of TEMPO reached 60% after 2 h at temperatures from 5 to 25 °C and 90% after another 5 h at 25 °C (Figure 1b). We suspected that BPO would also participate in this reaction to produce benzoate anions as side products. Indeed, after using 1 N aqueous NaOH solution to extract the benzoate anions from an ethyl ether solution, we obtained the *N*-alkoxyamine products (**A** and **OA**) after recrystallization from MeOH. The NMR spectra (Figure 2) of the *N*-alkoxyamines **A** and **OA** were identical to those described previously,[33,35,39,44] confirming the release of the benzoyloxyl radicals from BPO and radical addition with styrene and TEMPO. The protons labeled H$_c$, H$_d$, and H$_e$ from styrene in the *N*-alkoxyamine (**A**) and 4-oxo-*N*-alkoxyamine (**OA**) products appeared as three AB quartets of

Scheme 3. Synthetic Route toward PCL-*b*-P4VP Block Copolymer-Mediated Au NPs: (a) Redox-Induced Decomposition of BPO; (b) Radical Addition and Alcohol Oxidation; (c) Synthesis of PCL-*b*-P4VP; (d) Incorporation of Au NPs
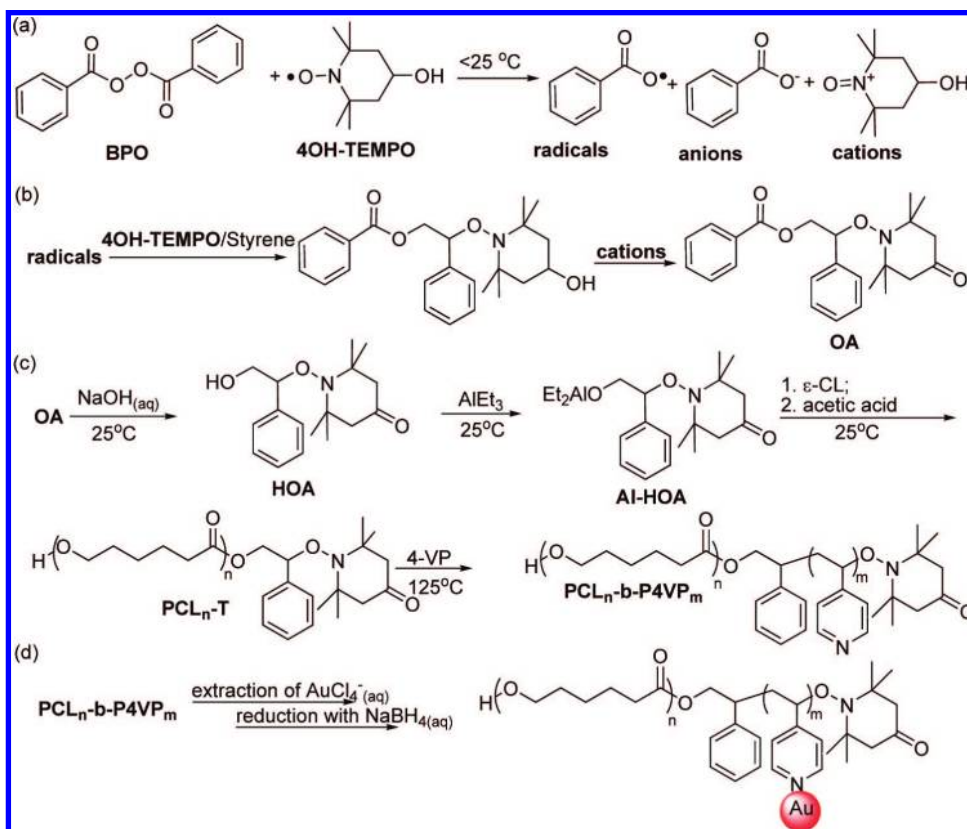
Scheme 4. Diethylaluminum Alkoxide-Induced ROP of *ε*-CL in the Presence of AlEt₃
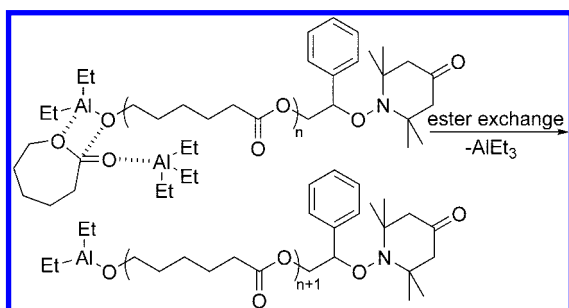
benzylic protons at 4.50−5.20 ppm in Figure 2a, providing direct evidence for the radical addition having occurred at such low temperatures (<25 °C). In comparison with the results of a previous study,[44] only the 4-oxo-*N*-alkoxyamines **OA** was obtained when using 4-OH-TEMPO. Because crystals of **OA** are insoluble in MeOH, it is easy to purify these compounds through precipitation. Upon recrystallization from the filtrate, we obtained a mixture of *N*-hydroxy-4-oxo-2,2,6,6-tetramethylpiperidine (*N*-hydroxylamine) and 2,6-dimethyl-6-nitrosohept-2-en-4-one (nitroso compound), which we identified using ¹H NMR and FTIR spectroscopy and mass spectrometry (Figure 3).

Nitroxide-Induced Alcohol Oxidation. In addition to NMRP, cyclic nitroxide free radicals (e.g., TEMPO and 4-OH-TEMPO) can also be used as catalysts for the oxidation of alcohols, for example, in the oxidation of alcohols using *m*-chloroperbenzoic acid (*m*-CPBA).[46,47] Cella et al. observed 4-oxo-TEMPO and 4-oxo-*N*-ammonium cations as side products when they used 4-OH-TEMPO in the nitroxide-catalyzed oxidation of alcohols with *m*-CPBA.[46] In the mechanism of nitroxide-catalyzed

alcohol oxidation,[48] one electron is transferred from TEMPO or 4-OH-TEMPO to *m*-CPBA, resulting in *N*-oxoammonium cations, which behave as efficient oxidants (not *m*-CPBA) to produce *N*-hydroxyamines and the corresponding aldehyde or ketone. The activated *m*-CPBA, with its additional electron, should decompose into the *m*-chlorobenzoyloxyl radical and hydroxide. Excess *m*-CPBA can also react with *N*-hydroxyamines to regenerate *N*-oxoammonium cations, and therefore, the relatively low amounts of TEMPO and 4-OH-TEMPO behave catalytically. We suggested that the reaction between BPO and TEMPO proceeds through a similar one-electron transfer and heterogeneous decomposition to give benzoyloxy radicals, the benzoate anion, and *N*-oxoammonium cations (Scheme 2a). Thus, *N*-alkoxyamine products can be obtained at temperatures below 25 °C through radical addition of the benzoyloxy radical with styrene and TEMPO (Scheme 2b). The side products of the *N*-oxoammonium cations are well-known strong organic oxidants[48] (Scheme 2c), and these unstable (ring strain) cations could undergo intermolecular rearrangement with benzoate anions to give a nitroso compound (Scheme 2d).[49] In the presence of the stable nitroxide free radical 4-OH-TEMPO, we attribute the formation of the 4-oxo-*N*-alkoxyamine **OA** to oxidation with the *N*-oxoammonium cation. Therefore, the 4-oxo-*N*-oxoammonium cation can be converted to *N*-hydroxy-4-oxo-2,2,6,6-tetramethylpiperidine through alcohol oxidation or to 2,6-dimethyl-6-nitrosohept-2-en-4-one through ring-opening rearrangement with benzoate anions (Figure 3). According to Langhals' study, the pale green color observed in the photograph in >Figure 1b corresponds to the UV−vis absorbance of 2,6-dimethyl-6-nitrosohept-2-ene (nitroso compound) at 685 nm.[49]

Temperature Effect. In the study reported by Yin et al.,[44] 4-hydroxyl- and 4-oxo-*N*-alkoxyamine products were obtained in 8.6% and 18.5% yields after heating BPO and 4-OH-TEMPO
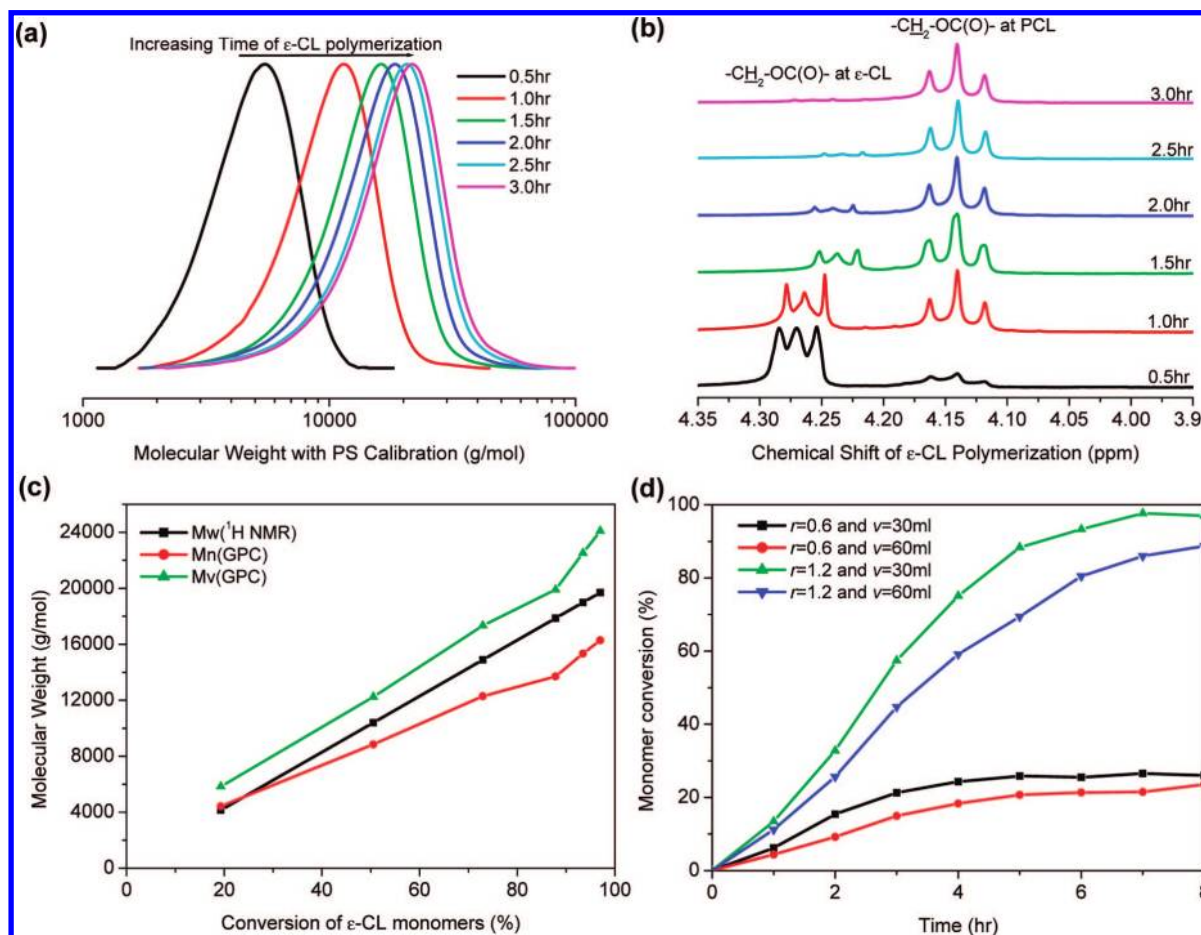
Figure 5. Aluminum alkoxide-initiated ROP of ε-CL leading to PCL (5 g, 20 000 g/mol): (a) GPC traces, (b) ^{1}H NMR spectra, and (c) molecular mass comparison of polymerization ($r = 1.5$; $v = 30$ mL); (d) monomer conversions at values of r of 0.6 or 1.2 and values of v of 30 or 60 mL.

Table 1. Compositions, Molecular Mass Distributions, and Thermal Properties of PCL Macroinitiator PCL and PCL-*b*-P4VP Diblock Copolymers BC1−3 and Au-BC1−3

	composition PCL$_n$-*b*-P4VP$_m$			molecular mass distribution				thermal properties				
								T_d,[e] °C	char yield,[e] wt %	T_g,[f] °C		T_m,[f] °C
entry	n^a	m	n/m^b	M_w,[c] g/mol	M_n,[d] g/mol	M_v,[d] g/mol	PDI[d]	5 wt % loss	at 700 °C	PCL	P4VP	PCL
PCL	175	0		20 000	16 700	20 200	1.21	299	0.5	−58		54
BC 1	175	44	3.99	24 900	19 000	24 600	1.29	291	0.3	−57	140	53
BC 2	175	75	2.16	28 800	21 700	28 600	1.32	289	2.16	−59	134	54
BC 3	175	117	1.50	32 600	21 300	29 700	1.40	296	2.65	−54	132	55
Au-BC 1								253	16.08			
Au-BC 2								213	15.18			
Au-BC 3								223	15.79			

^{a} Obtained from kinetic studies of ^{1}H NMR spectra, where n and m are the number of repeat units for the PCL and P4VP blocks, respectively. ^{b} Obtained from integration of the signals at 4.14 and 6.39 ppm in the ^{1}H NMR spectra for the PCL and P4VP blocks, respectively. ^{c} Calculated using the expression $nM_{\varepsilon\text{-CL}}$ (114.1 g/mol) + $mM_{4\text{-VP}}$ (105.1 g/mol) + $M_{\text{initiator}}$ (291.4 g/mol). ^{d} Obtained from GPC trace (eluent: DMF; 0.6 mL/min; PS-standard calibration): M_n, number-average molecular mass; M_v, molecular mass with the highest RI intensity; PDI, molecular mass distribution. ^{e} Obtained from TGA thermograms recorded at a heating rate of 20 °C/min. ^{f} Obtained from second-run DSC thermograms recorded at a heating rate of 20 °C/min.

in styrene at 80 °C. In contrast, we obtained only the 4-oxo-*N*-alkoxyamine in 37% yield at temperatures below 25 °C. When we added 5 equiv of an alcohol to a solution containing BPO, TEMPO, and styrene, we found that the conversion of the alcohol—determined using ^{1}H NMR spectroscopy (Table S1)—was less than 20%, i.e., equal to the TEMPO content (Figure 4). In this reaction, the conversion of the alcohol through oxidation depends on the concentration of *N*-oxoammonium cations.[48] In the presence of excess BPO, we suspect that *N*-oxoammonium cations were generated through a redox reaction between BPO and TEMPO, although BPO is not a sufficiently strong oxidant to regenerate *N*-oxoammonium cations from *N*-hydroxylamines. Therefore, the *N*-oxoammo-

nium cations could not oxidize all of the 4-hydroxyl-*N*-alkoxyamines, resulting in a mixture of 4-hydroxyl-*N*-alkoxyamine and 4-oxo-*N*-alkoxyamine products when some of the BPO decomposed thermally at 80 °C. Our proposed reaction mechanism suggests that some nitroxyl radicals are converted into *N*-oxoammonium cations during the bimolecular initiation for NMRP. Thus, unimolecular initiation is a better choice for preparing PCL-*b*-P4VP diblock copolymers so as to avoid inactive polymer chains.[13] During NMRP, the high mobility of the nitroxyl moiety is a very important factor of the rapid combination reaction between propagating free radical and nitroxyl radicals for the well-controlled living polymerization. Therefore, a more efficient ROP of ε-CL is initiated from the
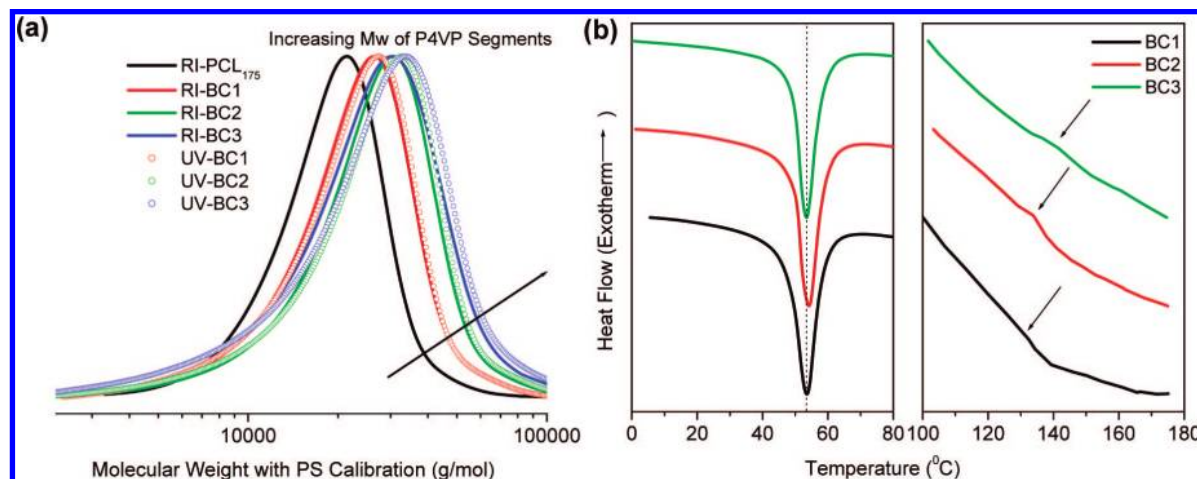
Figure 6. (a) GPC traces (RI and UV dual detection) of the **PCL** and the **BC1-3** and (b) DSC thermograms of the **BC1-3**: PCL melting transition (left) and P4VP glass transition (right).
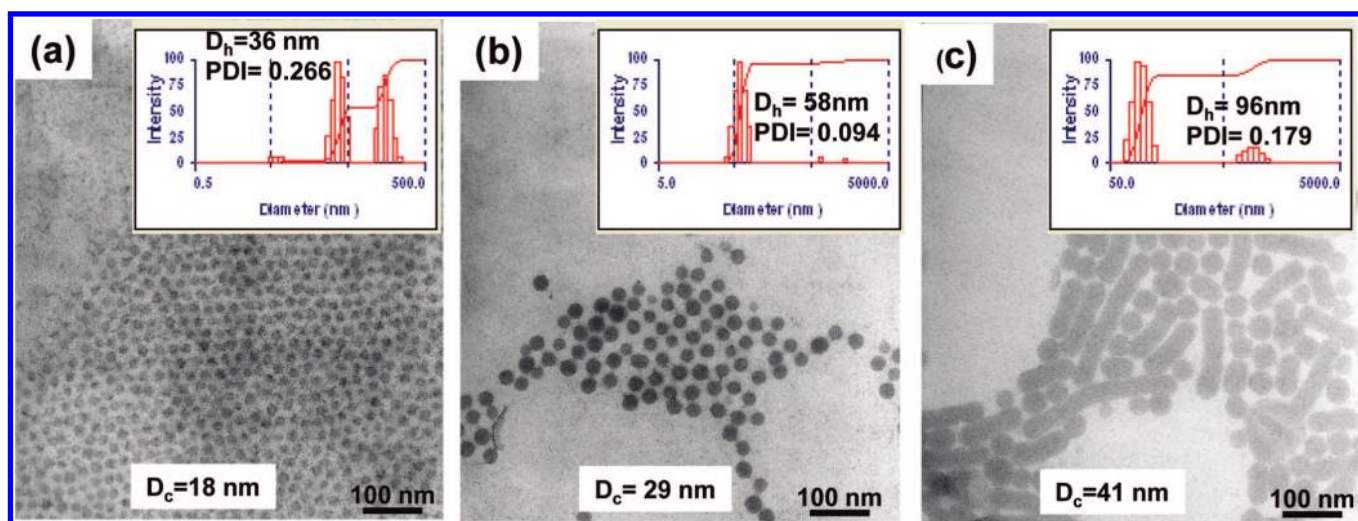

Figure 7. TEM images and inserted DLS graphs of PCL-*b*-P4VP diblock copolymer micelles (1 mg/mL) in a solvent of 10% DCM and 90% toluene (v/v) under stirring for 1 h: (a) **BC1**, (b) **BC2**, and (c) **BC3**.

OH groups on the carbon-centered fragments rather than the nitroxyl moieties. We selected the low-cost and commercially available 4-OH-TEMPO to prepare the hydroxyl-4-oxo-*N*-alkoxyamine **HOA** for use as a difunctional initiator in the synthesis of PCL-*b*-P4VP because all of the OH groups of 4-OH-TEMPO are oxidized and the products **OA** and **HOA** are very easily obtained.

PCL Macroinitiators. After hydrolysis of the benzoate ester on the 4-oxo-*N*-alkoxyamine **OA**, the dual (or double-headed) product, the hydroxyl-4-oxo-*N*-alkoxyamine **HOA**, contains a single primary alcohol, which is used as the initiating center for the living ROP of cyclic lactones, and a secondary benzylic group, which is an efficient initiator for the nitroxide-mediated "living" free radical polymerization of vinyl monomers. Scheme 3b depicts the ROP of ε-CL after the hydroxyl-4-oxo-*N*-alkoxyamine **HOA** had reacted with AlEt$_3$. Three types of aluminum alkoxides—AlEt$_2$OR, AlEt(OR)$_2$, and Al(OR)$_3$—may be formed in this step; living chain propagation succeeds through ester exchange with the ε-CL monomers. Because excess AlEt$_3$ can coordinate with the C=O groups on the ε-CL monomers to promote ester exchange (Scheme 4),[50] at a high ratio ($r = 1.5$) of AlEt$_3$ to **HOA**, most of the products were in the form AlEt$_2$OR, the propagation rate of which is the highest because of the low degree of steric hindrance for the approach of the next ε-CL monomer. The GPC trace for the product of ε-CL polymerization (Figure 5a) displays a shift in the molar mass

distribution to higher molecular mass upon increasing the degree of monomer conversion. The presence of trace amounts of AlEt(OR)$_2$ and Al(OR)$_3$, with their low propagation rates, may have resulted in PCL chains of lower molecular mass (i.e., the chromatographic tail). The ^{1}H NMR spectrum (Figure 5b) of the product of PCL polymerization (a dilute solution in CDCl$_3$ containing a trace of acetic acid) exhibits two signals at 4.24 and 4.14 ppm for protons on the carbon atoms adjacent to oxygen atoms, corresponding to cyclic monomers and linear polymers, respectively, indicating that complete conversion (>99.5%) occurred after 3 h. Therefore, we expected that upon increasing the conversion the number-average molecular mass (M_n in Figure 5a) would deviate from the theoretical values (M_w), which we calculated from ^{1}H NMR spectra (Figure 5b), as indicated in Figure 5c. In contrast, the maximum intensity (M_v) of the molecular mass distribution would agree with M_w; this trend provides evidence for a living PCL polymerization in which most of the ε-CL monomers are inserted from reactions with AlEt$_2$OR species. Thus, the presence of AlEt(OR)$_2$- or Al(OR)$_3$-initiated low-molecular-mass PCL chains result in the deviation of the GPC-obtained values of M_n from the ^{1}H NMR spectroscopy-derived values of M_w at high monomer conversions. At a lower AlEt$_3$ content ($r = 1.2$), fewer monomers become activated and PCL polymerization requires more time (ca. 8 h) to reach completion. In contrast, when r is equal to 0.6, the AlEt(OR)$_2$- and Al(OR)$_3$-initiated PCLs form gels at
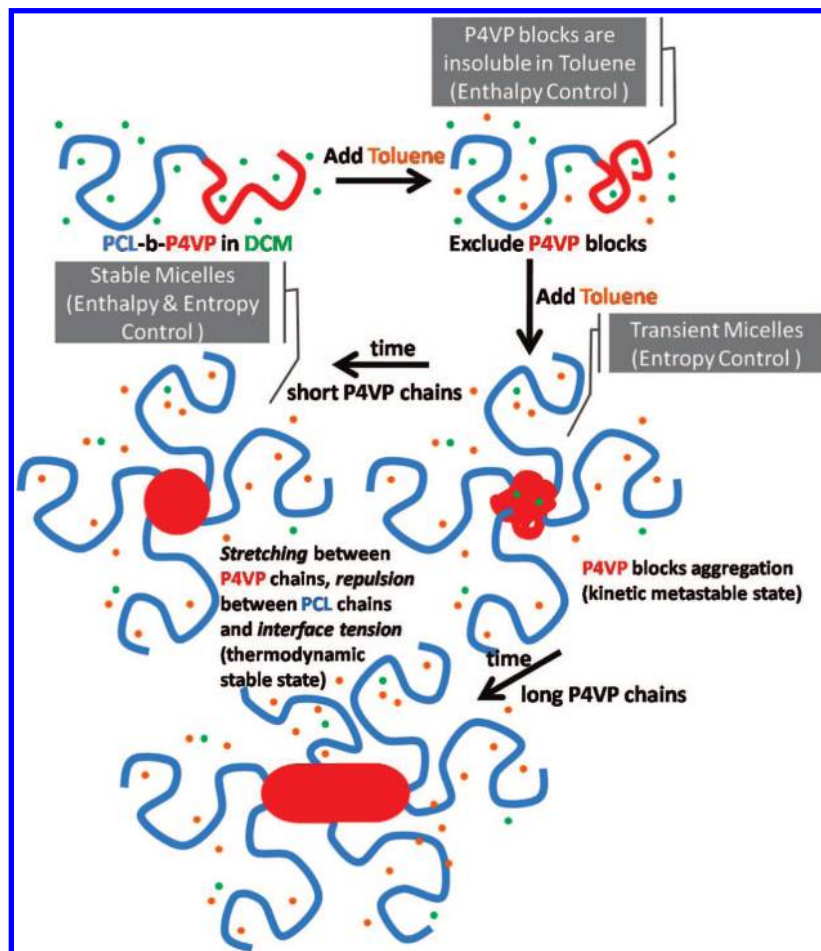
Figure 8. Schematic self-assembly mode of PCL-*b*-P4VP copolymers in toluene/DCM (90/10 v/v).
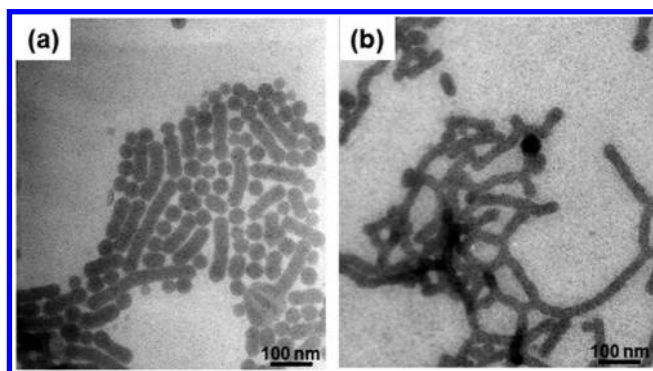

Figure 9. TEM images of **BC3** micelles (1 mg/mL) in toluene/DCM (90/10 v/v) under stirring for (a) 1 h and (b) 24 h.

ca. 20% conversion because they exist in the form of two- or three-arm high-molecular-mass star polymers prior to cleavage of the Al−OR bonds with glacial AcOH. By adding 2 equiv of toluene ($r = 0.6$; $v = 60$), the reaction rates are depressed as a result of a dilution effect, and the ultimate conversion also stops at 20%, as indicated in Figure 5d.

PCL-*b*-P4VP Copolymer. Under conditions where r and v are 1.5 and 30 mL, respectively, the high conversion of PCL polymerization (>99.5%) for 20 000 g/mol PCL allows the bulk NMRP immediately at 125 °C (without precipitation with MeOH) after deactivation of aluminum alkoxide with glacial AcOH, followed by vacuum distillation of toluene and replacement with the 4-VP monomer. After another 20 h, the solution becomes a gel (immobilizing the magnetic stirrer), which is a direct indication of diblock copolymer formation. Table 1 lists
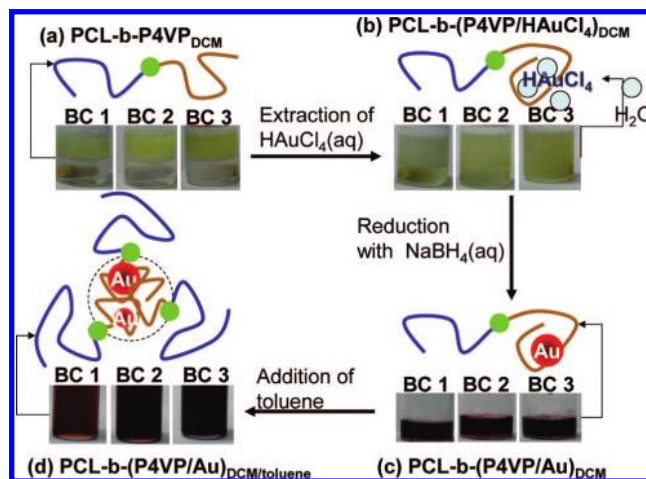

Figure 10. Schematic route toward the preparation of PCL-*b*-P4VP-protected Au NPs (**Au-BC1−3**): (a to b) two-phase extraction of HAuCl₄ via ion pairs NH⁺···AuCl₄⁻; (b to c) reduction with aqueous NaBH₄ solution; and (c to d) stabilization of Au NPs in the micellar cores upon the addition of excess toluene.

the compositions of the as-synthesized PCL-*b*-P4VP diblock copolymers (**BC1−3**) and their thermal properties. For homopolymerization of poly(4-vinypyridine) by NMRP, the conversion of the monomers was ca. 50%.[34] Even when adding 1, 2, or 4 equiv of 4-VP monomers by weight, the conversions of the three bulk NMRPs were relatively low (23%, 20%, and 15% for **BC1−3**, respectively) because the *N*-alkoxyamine end groups are restricted in the P4VP domain, which is segregated from the PCL block because of their immiscibility. Figure 6a
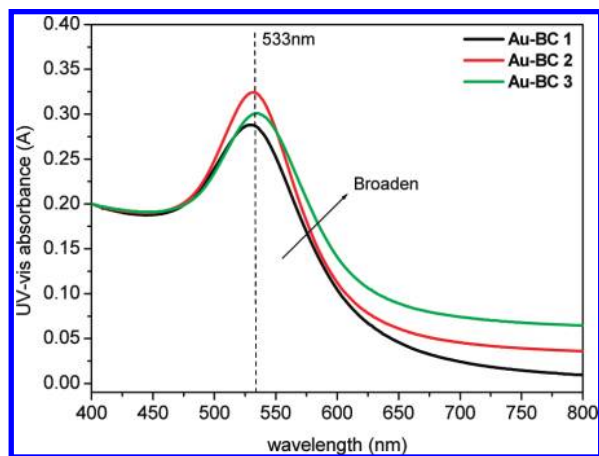
Figure 11. UV−vis spectra of Au NPs located in the micellar cores of three PCL-*b*-P4VP copolymers (**Au-BC1−3**).

indicates that the RI signals (unbroken lines) in the GPC traces shifted to higher molecular mass after the addition of more 4-VP monomer, especially in the high-molecular-mass region. The arene-sensitive UV signals (dashed lines) of the three PCL-*b*-P4VP diblock copolymers are coincident with those of the density-sensitive RI detector, indicating that all of the 4-VP monomers had been inserted from the *N*-alkoxyamine end groups of the PCL macroinitiator. Upon increasing the molecular mass, deviation of the UV- and RI-derived signals resulted from more 4-VP units being present in the high-molecular-mass PCL-*b*-P4VP diblock copolymers (e.g., in **BC3**). This behavior for the living P4VP polymerization is fully consistent with the insertion of the 4-vinylpyridine monomer units from the *N*-alkoxyamine end groups of the PCL macroinitiators. ^{1}H NMR spectra confirmed the diblock copolymer composition; Table 1 presents the integral areas of the signals at 4.14 and 6.39 ppm for the two protons on the PCL and P4VP repeat units, respectively.

Chemical dissimilarity between two blocks often confers an amphiphilic character to be used as polymeric surfactants. When dispersed in a selective solvent, which is compatible with PCL block but not with the other, asymmetric thermodynamic interactions lead to the formation of nanodomains with dimensions comparable to the molecular dimensions.[51] Although NMRP cannot control the molecular weight distribution as well as anionic polymerization ($M_w/M_n < 1.10$), TEM images revealed that the three PCL-*b*-P4VP diblock copolymers **BC1−3** possessed regular star micellar structures with smooth and distinct boundaries—i.e., spheres for **BC1** and **BC2**; spheres and rods with hemispherical caps for **BC3**—in the good solvent (toluene) for only the PCL block. Bedejacq et al. also found that the polystyrene-*b*-poly(acrylic acid) diblock copolymers ($M_w/M_n > 2$) can form the well-ordered microdomain structures in the bulk state.[52] DLS analysis of the PCL-*b*-P4VP diblock copolymers **BC1−3** in toluene/DCM (Figure 7) exhibited average micellar sizes (D_h) of 36, 58, and 87 nm, respectively, and polydispersity indices of 0.266, 0.094, and 0.179, respectively. TEM images of the RuO$_4$-stained PCL-*b*-P4VP diblock copolymers **BC1−3** revealed average core sizes (D_c) of 18, 29, and 41 nm due to the increase of P4VP block length. This observation indicates that the propagation of P4VP blocks initiate from the PCL macroinitiators to give the PCL-*b*-P4VP copolymers without P4VP homopolymers. Thus, the PCL-*b*-P4VP copolymer can form the smooth boundary of micelles through self-assembling P4VP chains in the core region (>Figure 8). Both PCL and P4VP blocks are soluble in dichloromethane (DCM, green dots), showing DCM-swelled polymeric chains. When adding toluene (brown dots), the P4VP blocks are excluded from the solvent

mixture due to the thermodynamic disfavor with toluene. When the length of PCL is very long, the repulsive interactions among intercoronal chains exceed the interfacial energies and dominate the equilibrium structure. As adding more toluene, the P4VP blocks are quickly segregated into the separated phase (transient micelles) to reduce the interface area with toluene, but the stable micelles with thermodynamic stable state need time to balance three interactions: stretching between aggregated P4VP chains, repulsion between DCM-swelled PCL chains, and interface tension between P4VP and PCL domains.[13,53] When the volume fractions of P4VP domains are larger than 0.3, the solution morphology of PCL-*b*-P4VP shifts from spheres to rods in toluene/DCM (90/10 v/v). As the length of the P4VPis increased, the core chain stretching becomes relatively significant and can be suppressed by connecting spheres to form smooth rods with hemisphereical caps.[54] Meanwhile, the repulsion between PCL chains and the interface tension can be also decreased. In addition, the increase of PCL shell thickness from 18 to 29 nm and to 46 nm for **BC1**, **BC2**, and **BC3** results from stretching PCL corona chains. As a result, the coexistence of spherical and rodlike structures of **BC3** with low total interfacial energies is favored rather than spherical micelles such as **BC1** and **BC2**. It is believed that rodlike micelles are formed by collision of the spherical micelles followed by fusion. Thus, the coexistence of spherical and rodlike micelles can be attributed to at least two factors. First, a lack of communication between spherical micelles results in long-lived metastable structures. Second, polydispersity, an inevitable consequence of synthetic techniques, may contribute as well.[51,55,56] In comparison with TEM images in Figure 9, the more rodlike morphology for a long-term of stirring indicates that a lack of communication between spherical micelles mainly results in the coexistence microstructures in Figure 7c.

PCL-*b*-P4VP Copolymer-Protected Au NPs. To remove heavy metal ions from wastewater through simple filtration separation, coagulation of metal-binding polymers is required. In this case, the hydrophobic PCL block plays an important role during the two-phase extraction because the metalated P4VP block with an ionic bond of $NH^+ \cdots AuCl_4^-$ becomes amphiphilic,[57] which would emulsify partial copolymers possessing short-chain PCL blocks, resulting in turbid aqueous solutions (see, for example, the upper layer of the inserted graphs after extraction of HAuCl$_4$ in Figure 10). For the organic phase, we can also recycle metal ions in the form of NPs through chemical reduction. As indicated in Scheme 3d and Figure 10, an equimolar amount of AuCl$_4^-$ anions (with respect to pyridine units) can be added to transfer from water to DCM through ionic interactions with the protonated pyridyl groups (i.e., $NH^+ \cdots AuCl_4^-$). The miscible of P4VP block in DCM was deteriorated due to the excess amounts of HAuCl$_4$ at which the accommodation of coordination reached maximum allowance and thus led to the occurrence of solubility limit.[24] Therefore, the organic phase [see, for example, the bottom layer of the inserted graphs after extraction of HAuCl$_4$ in Figure 10b] became slightly turbid and yellowish because the $NH^+ \cdots AuCl_4^-$ ion pairs transported some water molecules, which provided a medium to react with NaBH$_4$ in the aqueous solution and remove the byproduct HCl$_{(aq)}$ (deprotonation of 4VP units) from the organic phase after reduction. Protonation of P4VP blocks might result in swelling of the micelle cores (fully protonated P4VP is soluble in water) due to increase in osmotic pressure.[57−59] After adding excess toluene, the diblock copolymer micelles could store the Au NPs in their cores, resulting in a transparent reddish solution. Figure 11 displays UV−vis spectra of Au NPs in the cores of the PCL-*b*-P4VP micelles **Au-BC1−3**; we observe typical surface plasmon behavior for the Au NPs, with maximum intensity at 533 nm. The signal maximum did not
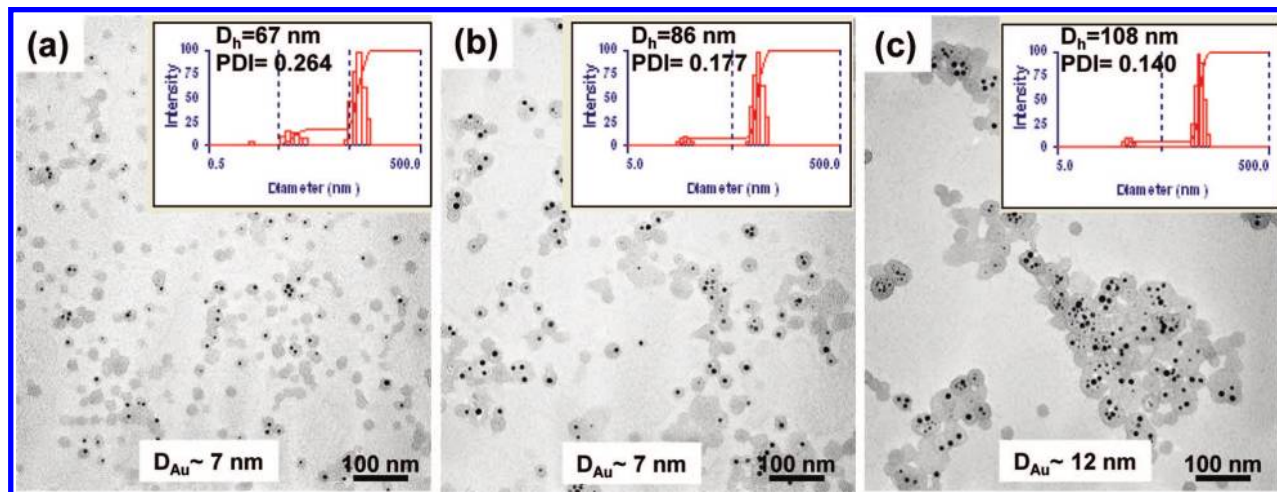
Figure 12. TEM images and inserted DLS graphs of Au NPs located in the micellar cores of three PCL-*b*-P4VP copolymers: (a) **Au-BC1**, (b) **Au-BC2**, and (c) **Au-BC3**.

shift to higher wavelength (red shift) for the larger Au NPs, but the signal did broaden. The broad UV−vis signal for **Au-BC3** corresponds to the larger size of Au NPs (ca. 12 nm) in comparison with those (ca. 7 nm) for **Au-BC1** or **Au-BC2**, as determined from the TEM images displayed in Figure 12.

At the equimolar ratio of $HAuCl_4$ to 4-VP units, the more Au NPs can be incorporated to the longer P4VP chains of **BC3** resulting in the morphologic transform from rodlike **BC3** to spherical **Au-BC3** (Figure 7c and Figure 12c). Not surprisingly, metalation suppress regular aggregation of the PCL-*b*-P4VP micelles due to the complexation of the P4VP blocks with spherical Au NPs.[24] DLS analysis of the Au NPs in the cores of the PCL-*b*-P4VP micelles **Au-BC1−3** in toluene/DCM (Figure 12) revealed average micellar sizes (D_h) of 67, 86, and 108 nm, respectively, and polydispersity indices of 0.264, 0.177, and 0.140, respectively. From a comparison with the sizes of the PCL-*b*-P4VP micelles **BC1−3** in Figure 7>, we attribute the increases in the micelle sizes of 31, 28, and 21 nm for **Au-BC1−3**, respectively, to the incorporation of the 7−12 nm diameter Au NPs in the P4VP cores. In addition, the absence of large Au aggregates (>50 nm in diameter) in the TEM images reveals that the P4VP blocks not only captured the $AuCl_4^-$ anions in form of $NH^+ \cdots AuCl_4^-$ complexes but also stabilized the Au NPs through the formation of metal complexes. We quantitatively calculated the capacities of the Au NPs relative to PCL-*b*-P4VP block copolymers **BC1−3** to be 0.19, 0.15, and 0.16 g/g for **Au-BC1−3**, respectively, deduced from the char yield at 700 °C (Table 1 and Figure S9).

Conclusions

Benzoyloxyl radicals can be produced through TEMPO-induced BPO decomposition at temperatures below 25 °C. Thus, the preparation of *N*-alkoxyamine unimolecular initiators for nitroxide-mediated radical polymerizations becomes easier because radical side reactions seldom occur at such low temperatures. As a result, the ability to control polymer properties through the synthesis of diblock copolymers and complex macromolecular architectures becomes cheaper and simpler for the preparation of *N*-alkoxyamine products. Active byproducts of the *N*-oxoammonium cations would undergo alcohol oxidization to produce *N*-hydroxylamines or ring-opening rearrangement to form nitroso compounds. Thus, during this process, we observed a color change for the solution from reddish brown (nitroxide absorbance) to pale green (nitroso absorbance). When using the cheaper 4-OH-TEMPO, we prepared only 4-oxo-*N*-alkoxyamine products through a process

involving redox reaction, radical addition, and alcohol oxidation. After hydrolysis of the benzoate ester, the hydroxyl-4-oxo-*N*-alkoxyamine can be used as a difunctional initiator for the preparation of PCL-*b*-P4VP diblock copolymers through (i) ring-opening polymerization of ε-CL after reaction with $AlEt_3$ and (ii) bulk nitroxide-mediated radical polymerization of 4-VP. When using 1.5 equiv of $AlEt_3$, diethylaluminum alkoxide initiation and the presence of more active monomers can lead to the conversion of ε-CL monomer reaching 99.5% after 3 h in toluene at 25 °C; as a result, the preparation of PCL-*b*-P4VP can be performed at 125 °C after replacing the toluene solvent with 4-VP monomers. The immiscible PCL-*b*-P4VP diblock copolymers display not only two distinct glass transitions in the DSC thermograms but also unique micellar structures, such as spheres or rods, in the TEM images. Using this combination of ROP and NMRP, we prepared three PCL-*b*-P4VP copolymers having polydispersities of 1.29−1.40 that retained the desired characteristics of a uniform P4VP core size in a mixed solvent of 10% DCM and 90% toluene (v/v). The relative block length plays an important role in affecting the resulting supramolecular architecture. Depending on the diblock ratio *n/m*, the **BC1** and **BC2** diblock copolymers initially formed spheres (*n/m* = 3.99, 2.16) and then shifted to a mixture of spheres and rods (*n/m* = 1.50). For the extraction of $HAuCl_4$ from aqueous solution, $AuCl_4^-$ anions were transferred into DCM in the form of ionic pairs ($NH^+ \cdots AuCl_4^-$), which then were stabilized in the form of Au NPs through reduction with aqueous $NaBH_4$ solution.

Supporting Information Available: Experimental details. This material is available free of charge via the Internet at http://pubs.acs.org.

References and Notes

(1) Shannon, M. A.; Bohn, P. W.; Elimelech, M.; Georgiadis, J. G.; Mariñas, B. J.; Mayes, A. M. *Nature (London)* **2008**, *452*, 301.
(2) Rahman, M. A.; Ahsan, S.; Kaneco, S.; Katsumata, H.; Suzuki, T.; Ohta, K. *J. Environ. Manage.* **2005**, *74*, 107.
(3) Akthakul, A.; Salinaro, R. F.; Mayes, A. M. *Macromolecules* **2004**, *37*, 7663.
(4) Zhou, M.; Kidd, T. J.; Noble, R. D.; Gin, D. L. *Adv. Mater.* **2005**, *17*, 1850.
(5) Asatekin, A.; Menniti, A.; Kang, S.; Elimelech, M.; Morgenroth, E.; Mayes, A. M. *J. Membr. Sci.* **2006**, *285*, 81.
(6) Revanur, R.; McCloskey, B.; Breitenkamp, K.; Freeman, B. D.; Emrick, T. *Macromolecules* **2007**, *40*, 3624.

(7) Yang, S. Y.; Ryu, I.; Kim, H. Y.; Kim, J. K.; Jang, S. K.; Russell, T. P. *Adv. Mater.* **2006**, *18*, 709.

(8) Phillip, W. A.; Rzayev, J.; Hillmyer, M. A.; Cussler, E. L. *J. Membr. Sci.* **2006**, *286*, 144.

(9) Förster, S.; Plantenberg, T. *Angew. Chem., Int. Ed.* **2002**, *41*, 688.

(10) Zhang, L.; Eisenberg, A. *Science* **1995**, *268*, 1728.

(11) Zhang, L.; Eisenberg, A. *J. Am. Chem. Soc.* **1996**, *118*, 3168.

(12) Zhang, L.; Yu, K.; Eisenberg, A. *Science* **1996**, *272*, 1777.

(13) Chan, S. C.; Kuo, S. W.; Lu, C. H.; Lee, H. F.; Chang, F. C. *Polymer* **2007**, *48*, 5059.

(14) Konya, Z.; Puntes, V. F.; Kiricsi, I.; Zhu, J.; Ager, J. W., III; Ko, M. K.; Frei, H.; Alivisatos, P.; Somorjai, G. A. *Chem. Mater.* **2003**, *15*, 1242.

(15) Lin, S. D.; Bollinger, M.; Vannice, M. A. *Catal. Lett.* **1993**, *17*, 245.

(16) Lee, S. J.; Gavriilidis, A. *J. Catal.* **2002**, *206*, 305.

(17) Okumura, M.; Akita, T.; Haruta, M. *Catal. Today* **2002**, *74*, 265.

(18) Sárkány, A.; Horváth, A.; Bech, A. *Appl. Catal., A* **2002**, *229*, 117.

(19) Milone, C.; Tropeano, M. L.; Gulino, G.; Neri, G.; Ingoglia, R.; Galvagno, S. *Chem. Commun.* **2002**, 868.

(20) Blick, K.; Mitrelias, T. D.; Hargreaves, J. S. J.; Hutchings, G. J.; Joyner, R. W.; Kiely, C. J.; Wagner, F. E. *Catal. Lett.* **1998**, *50*, 211.

(21) Grisel, R. J. H.; Kooyman, P. J.; Nieuwenhuys, B. E. *J. Catal.* **2000**, *191*, 430.

(22) Salama, T. M.; Ohnishi, R.; Shido, T.; Ichikawa, M. *J. Catal.* **1996**, *162*, 169.

(23) Brust, M.; Walker, M.; Bethell, D.; Schiffrin, D. J.; Whyman, R. *J. Chem. Soc., Chem. Commun.* **1994**, 801.

(24) Ho, R. M.; Lin, T.; Jhong, M. R.; Chung, T. M.; Ko, B. T.; Chen, Y. C. *Macromolecules* **2005**, *38*, 8607.

(25) Azzam, T.; Eisenberg, A. *Langmuir* **2007**, *23*, 2126.

(26) Mössmer, S.; Spatz, J. P.; Möller, M. *Macromolecules* **2000**, *33*, 4791.

(27) Hou, G.; Zhu, L.; Chen, D.; Jiang, M. *Macromolecules* **2007**, *40*, 2134.

(28) Albertsson, A. C.; Varma, I. K. *Adv. Polym. Sci.* **2002**, *157*, 1.

(29) Stridsberg, K. M.; Ryner, M.; Albertsson, A.-C. *Adv. Polym. Sci.* **2002**, *157*, 41.

(30) Greszta, D.; Mardare, D.; Matyjaszewski, K. *Macromolecules* **1994**, *27*, 638.

(31) Matyjaszewski, K.; Xia, J. *Chem. Rev.* **2001**, *101*, 2921.

(32) Hawker, C. J.; Bosman, A. W.; Harth, E. *Chem. Rev.* **2001**, *101*, 3661.

(33) Sciannamea, V.; Jerome, R.; Detrembleur, C. *Chem. Rev.* **2008**, *108*, 1104.

(34) Fischer, A.; Brembilla, A.; Lochon, P. *Macromolecules* **1999**, *32*, 6069.

(35) Hawker, C. J.; Hedrick, J. L.; Malmström, E. E.; Trollsås, M.; Mecerreyes, D.; Moineau, G.; Dubois, Ph.; Jérôme, R. *Macromolecules* **1998**, *31*, 213.

(36) Hawker, C. J. *J. Am. Chem. Soc.* **1994**, *116*, 11185.

(37) Georges, M. K.; Veregin, R. P. N.; Kazmaier, P. M.; Hamer, G. K. *Macromolecules* **1993**, *26*, 2987.

(38) Moad, G.; Rizzardo, E.; Solomon, D. H. *Macromolecules* **1982**, *15*, 909.

(39) Gravert, D. J.; Janda, K. D. *Tetrahedron Lett.* **1998**, *39*, 1513.

(40) Moad, G.; Rizzardo, E.; Solomon, D. H. *Tetrahedron Lett.* **1981**, *22*, 1165.

(41) Moad, G.; Rizzardo, E.; Solomon, D. H. *J. Macromol. Sci., Chem.* **1982**, *A17*, 51.

(42) Veregin, R. P. N.; Georges, M. K.; Kazmaier, P. M.; Hamer, G. K. *Macromolecules* **1993**, *26*, 5316.

(43) Braslau, R.; Burrill, L. C., II; Siano, M.; Naik, N.; Howden, R. K.; Mahal, L. K. *Macromolecules* **1997**, *30*, 6445.

(44) Yin, M.; Wang, Y.; Bauer, I.; Habicher, W. D.; Voit, B. *Des. Monomers Polym.* **2005**, *8*, 211.

(45) Hawker, C. J.; Barclay, G. G.; Dao, J. *J. Am. Chem. Soc.* **1996**, *118*, 11467.

(46) Cella, J. A.; Kelley, J. A.; Kenehan, E. F. *J. Org. Chem.* **1975**, *40*, 1860.

(47) Rychnovsky, S. D.; Vaidyanathan, R. *J. Org. Chem.* **1999**, *64*, 310.

(48) Sheldon, R. A.; Arends, I. W. C. E.; ten Brink, G.-J.; Dijksman, A. *Acc. Chem. Res.* **2002**, *35*, 774.

(49) Fritz-Langhals, E. *Org. Process Res. Dev.* **2005**, *9*, 577.

(50) Dubois, Ph.; Ropson, N.; Jerome, R.; Teyssie, Ph. *Macromolecules* **1996**, *29*, 1965.

(51) Won, Y. Y.; Bates, F. S. In *Nonionic Block Compolymer Wormlike Micelles*; Zana, R., Kaler, E. W., Eds.; Surfactant Sciences Series; Taylor & Francis: New York, 2006.

(52) Benejacq, D.; Ponsinet, V.; Joanicot, M.; Loo, Y.-L.; Register, R. A. *Macromolecules* **2002**, *35*, 6645.

(53) Zhang, L.; Eisenberg, A. *J. Am. Chem. Soc.* **1996**, *118*, 3168.

(54) Burke, S. E.; Eisenberg, A. *Langmuir* **2001**, *17*, 6705.

(55) Lynd, N. A.; Hillmyer, M. A. *Macromolecules* **2005**, *38*, 8803.

(56) Listak, J.; Jakubowski, W.; Mueller, L.; Plichta, A.; Matyjaszewski, K.; Bockstaller, M. R. *Macromolecules* **2008**, *41*, 5919.

(57) Sidorov, S. N.; Bronstein, L. M.; Kabachii, Y. A.; Valetsky, P. M.; Soo, P. L.; Maysinger, D.; Eisenberg, A. *Langmuir* **2004**, *20*, 3543.

(58) Kostarelos, K.; Luckham, P. F.; Tadros, T. F. *J. Chem. Soc., Faraday Trans.* **1998**, *94*, 2159.

(59) Groenewegen, W.; Egelhaaf, S. U.; Lapp, A.; van der Maarel, J. R. C. *Macromolecules* **2000**, *33*, 3283.